Adapting the Förster Theory of Energy Transfer for Modeling Dynamics in Aggregated Molecular Assemblies

Gregory D. Scholes,[†] Xanthipe J. Jordanides, and Graham R. Fleming*

Department of Chemistry, University of California, Berkeley, California, and Physical Biosciences Division, Lawrence Berkeley National Laboratory, Berkeley, California 94720-1460

Received: September 29, 2000; In Final Form: December 5, 2000

The remarkable efficiencies of solar energy conversion attained by photosynthetic organisms derive partly from the designs of the light-harvesting apparatuses. The strategy employed by nature is to capture sunlight over a wide spectral and spatial cross section in chromophore arrays, then funnel the energy to a trap (reaction center). Nature's blueprint has inspired the conception of a diversity of artificial light-harvesting antenna systems for applications in solar energy conversion or photonics. Despite numerous, wide-ranging studies, truly quantitative predictions for such multichromophoric assemblies are scarce because Förster theory in its standard form often seems to fail. We report here a new framework within which energy transfer in molecular assemblies can be modeled quantitatively using a generalization of Förster's theory. Our results show that the principles involved in optimization of energy transfer in confined molecular assemblies are not revealed in a simple way by the absorption and emission spectra because such spectra are insensitive to length scales on the order of molecular dimensions.

I. Introduction

The transfer of electronic excitation energy from an excited molecule (or atom) to another, electronic excitation transfer (EET), is a fundamental physical process. For example, EET is used in natural and synthetic light-harvesting to funnel light from any point in the antenna to a trap—the reaction center.[1,2] EET can also effect photodegradation in macromolecules by transferring excitation energy to photochemical (impurity) traps.[3,4] There has been much recent interest in the design of supramolecular systems that utilize EET to direct energy flow.[5-10] To accompany such advances, new ideas need to be introduced to enable EET dynamics in confined chromophore aggregates to be understood. That is the purpose of the present paper.

A successful, widely employed quantitative method for calculating rates of EET between donor (D)−acceptor (A) pairs was developed by Förster.[11] Förster connected the energy released by deexcitation of D and that synchronously taken up by A to the emission and absorption line shapes, respectively. In the modern parlance of condensed phase spectroscopy, line shape refers to Franck−Condon progressions and line broadening of the transition energy caused by interactions between the molecule and its environment.[12,13] We furthermore define the homogeneous line broadening as that caused by fluctuations of the environment that are rapid compared to the time scale of the EET. Slow fluctuations, inhomogeneous line broadening, are manifest as static disorder in the transition energies. We address static disorder in section II.C. Förster wrote

$$k = \frac{2\pi}{\hbar} \int_0^\infty d\epsilon \sum_k \sum_l P(k)P(l)|u(\bar{\epsilon}_d^k, \bar{\epsilon}_a^l, \epsilon)|^2 \qquad (1)$$

where $\bar{\epsilon}_d^k$ is the energy gap of the donor molecule, adjusted according to $P(k)$ for thermal population of mode k in the excited state, and similarly for $\bar{\epsilon}_a^l$ with respect to the acceptor ground state. Owing to the normalization adopted by Förster,[11] the matrix element u is a dimensionless quantity. In the absence of static disorder, the energy conservation condition takes the simple form of an overlap between donor emission, $f^{hom}(\epsilon)$, and acceptor absorption, $a^{hom}(\epsilon)$, spectra which have each been normalized to unit area on an energy scale, $J(\epsilon) = f^{hom}(\epsilon)a^{hom}(\epsilon)$. Thus, eq 1 is rewritten as

$$k = \frac{2\pi}{\hbar}|V|^2 \int_0^\infty d\epsilon \, J(\epsilon) \qquad (2)$$

where V is the electronic coupling between donor and acceptor. In the usual representation of the Förster equation,[14] there is a further entanglement of electronic and nuclear factors which arises because the electronic coupling factor is obtained by combining the information contained in the Förster spectral overlap integral (see refs 15 and 16) $I(\bar{\nu})\phi_D/\tau_D \propto |\mu_D|^2 J(\bar{\nu})|\mu_A|^2$ with the κ^2/R^6 factor in the rate expression.

The Förster equation, as it stands, eq 2, is appropriate provided that four conditions are satisfied: (i) A dipole−dipole (or convergent multipole−multipole) approximation for the electronic coupling can be employed appropriately for the donor−acceptor interaction. (ii) Neither the donor fluorescence lifetime, emission line shape, acceptor absorption line shape, nor oscillator strength is perturbed because of interactions among donors or acceptors, respectively. (iii) Static disorder (inhomogeneous line broadening) is absent in the donor and acceptor line shapes. (iv) The energy transfer dynamics are incoherent.

The Förster theory for EET has proved successful for predicting rates of energy transfer based on the overlap of donor emission and acceptor absorption spectra.[15,17,18] However, when several donor and/or acceptor chromophores are arranged in a confined geometry, then eq 1 cannot necessarily be employed to model population dynamics following optical excitation. For

---

* Corresponding author. E-mail: GRFleming@lbl.gov.
† Present address: Lash Miller Chemical Laboratories, 80 St. George Street, University of Toronto, Toronto, Canada M5S 3H6. E-mail: gscholes@chem.utoronto.ca.
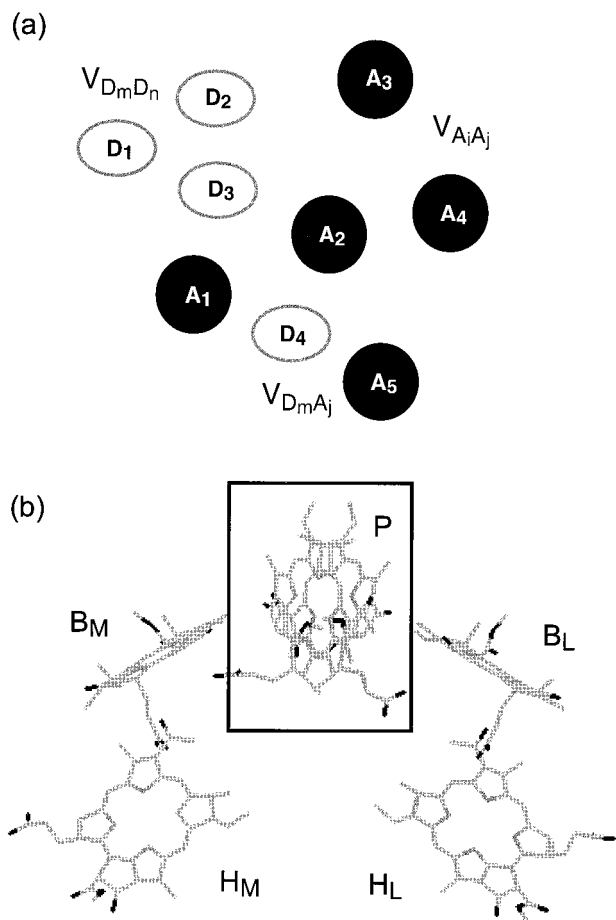
Förster Theory of Energy Transfer

J. Phys. Chem. B, Vol. 105, No. 8, 2001 **1641**

Figure 1. (a) Schematic depiction of a general aggregate comprised of several donor molecules (or atoms) D and acceptor molecules A. We indicate couplings between donors $V_{D_mD_n}$, couplings between acceptors $V_{A_iA_j}$, and couplings between donors and acceptors $V_{D_mA_j}$. (b) A specific example of such an aggregate: the purple bacterial photosynthetic reaction center. The dimer formed by the strongly interacting P_M and P_L bacteriochlorophyll molecules acts as an energy acceptor when any of the B or H molecules are electronically excited.

example, consider the molecular aggregate depicted in Figure 1a. EET in ordered systems, or aggregates, has been considered to proceed via three possible, distinct mechanisms:[19] (1) the "trivial" mechanism involving emission and reabsorption,[20] (2) resonance energy transfer between individual molecules,[11,21] and (3) the migration of excitons.[22,23] The dynamics associated with aggregates such as those depicted in Figure 1 are not always accommodated in any of these categories; it is more of an intermediate situation. There can be some strong couplings and some weak couplings among the various components. There are three distinct categories of electronic coupling evident: couplings between donors $V_{D_mD_n}$, couplings between acceptors $V_{A_iA_j}$, and couplings between donors and acceptors $V_{D_mA_j}$. If all these couplings are very weak as gauged against spectral line shapes, then a Förster-type pairwise energy hopping model adequately explains the excited state dynamics. However, if any of the couplings are sufficiently strong that spectral line shapes or radiative rates are perturbed, then eq 2 becomes inadequate. In general, a detailed description of the excited-state dynamics in such an aggregate is very complicated. In the present work we show that, provided the couplings $V_{D_mA_j}$ are weak, we can retain the ideas presented by Förster—though in modified form—and thus employ a relatively simple model to explore and to quantify EET dynamics in complex multichromophoric aggregates.

In 1942 London noted,[24] in connection with van der Waals forces, that when interacting molecules are large compared to their separation, the simple relationship between optical properties, such as dipole transition strengths, and electronic coupling fails. Such a failure of the dipole approximation is more than a slow convergence of the multipole expansion of the Coulomb interaction. In fact, the concept of a multipole expansion becomes meaningless; rather, local interactions between different parts of each molecule must be considered. For example, London[24] and others[25,26] have considered the transition density of each molecule to be better approximated by a set of virtual oscillators, distributed according to the geometry of the molecule. Recently we have simply used the transition densities without reduction.[27]

Valkunas and co-workers[28] extended these concepts to the calculation of EET rates between a monomer donor molecule and a large molecular J-aggregate acceptor. They found that, because the donor interacts most significantly with only a small part of the J-aggregate, electronic couplings are not proportional to the oscillator strength of the J-aggregate exciton states. Hence excitation energy may be readily accepted into exciton states of the J-aggregate that have no oscillator strength in the optical absorption spectrum. Recently Sumi[29] and ourselves[30] arrived independently at this same conclusion. In our recent work we took these basic concepts a step further, and considered the ensemble averaging component of the problem. Disorder in site energies of the molecules that make up an aggregate (i.e., energy offsets that persist for times longer than the EET time) can have profound implications for EET in aggregates, as we will explore further in the present work.

The key quantity that we will be concerned with is the *dimensionless* matrix element of the interaction, u, which governs the Förster spectral overlap. This u corresponds to the dimensionless quantity $|V|^2 J(\epsilon)$ of eq 2: the coupling-weighted spectral overlap. We will show how this quantity can be evaluated for complex systems. We will then go on to explain how this quantity can be used to elucidate the *mechanism* by which EET is promoted in complex aggregates. Moreover, when energetic disorder in the site energies of these chromophores is significant, we must rethink the ensemble averaging which underlies Förster theory. The central finding we report here is that the EET dynamics need to be calculated by considering a molecular picture of the aggregate, rather than identifying donors and acceptors merely as spectroscopic bands.

The results presented in this paper have general implications for quantifying EET in multichromophoric assemblies. Some concepts are not intuitive, so in order to describe these results more clearly we often refer to a specific application of the theory to the photosynthetic reaction center (RC) of purple bacteria. In the accompanying paper we report our detailed studies of EET dynamics in various different purple bacterial reaction centers, reinforcing the quantitative success and general applicability of the model.[31]

II. Energy Transfer in Molecular Aggregates

A. Rethinking the Meaning of the Dipole Approximation. One normally thinks of the multipolar expansion of the Coulombic interaction[32] as being convergent. In other words, the dipole—dipole coupling dominates for allowed transitions, with higher order interactions merely correcting slightly the value of this coupling; after all, they are more strongly attenuated with distance (R^{-5}, R^{-7}, etc.). Such a point of view was introduced by Dexter[21] and has persisted despite the development of the distributed monopole method[25,26] and the transition density cube (TDC) method.[27] While the multipole expansion
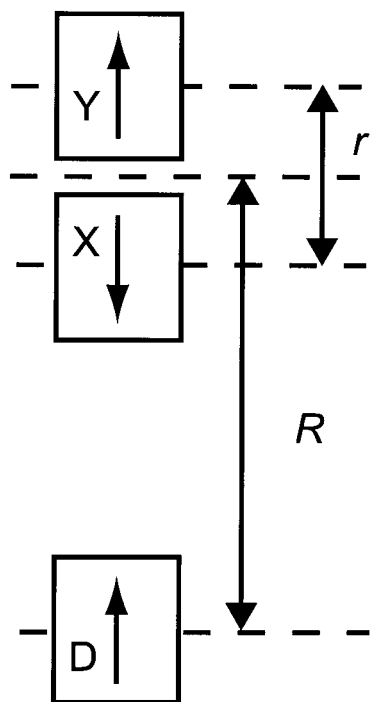
Figure 2. A depiction of the geomtrical arrangement of a hypothetical model aggregate consisting of a dimer formed by arranging molecules X and Y in a tail-to-tail orientation, and positioning molecule D a distance R from the center of the X−Y dimer.

way of thinking makes sense for atomic systems, it is not appropriate for electronic couplings between molecules because it averages away the shape of the donor and acceptor molecules. In other words, in order for the multipole expansion to converge, the size of the donor and acceptor molecules must be much smaller than the separation between them. So, if the definition of separation is ambiguous—for example, there is a significant difference between the center-to-center and edge-edge separations—then it is inadvisable to use a multipolar expansion of the Coulombic coupling.

We will take this reasoning a step further here, and suggest that when more than one donor and/or acceptor are coupled in a confined geometry, then the minimal representation is one that includes explicit account of each molecular center. Our point is easily illustrated by considering an example of a single donor D and a pair of acceptors X and Y, as depicted in Figure 2. Here the electronic coupling between D and the symmetric dimer acceptor state A_+ is, according to Förster theory with constants and orientation factors set to unity, eq 3a, where μ_+ is the transition moment of the state A_+, which in the example given is exactly zero. However, if the coupling is determined in terms of the molecular composition of $A_+ = (|X^*Y\rangle + |XY^*\rangle)/\sqrt{2}$, but still using the dipole approximation for site−site couplings, then we obtain eq 3b,

$$V = \mu_D \mu_+ / R^3 = 0 \tag{3a}$$

$$V = [\mu_D \mu_X / (R - r)^3 - \mu_D \mu_Y / (R + r)^3] / \sqrt{2} \neq 0 \tag{3b}$$

The difference between the electronic coupling obtained using eq 3b compared to eq 3a is particularly significant when r (the center-to-center separation between the two acceptor molecules) and R (the center-to-center separation between the donor and the acceptor dimer) are similar.

When the donor and acceptor molecules are closely located relative to molecular dimensions, then the analogy between

synergistic absorption and emission processes and the Coulombic interaction (i.e., the Förster-Dexter picture) breaks down. This is because local interactions between the donor and acceptor transition densities can overwhelm the overall coupling. In such a case there is a distinct and important difference between averaging over wave functions, then coupling them, as we did in eq 3a using eq 4a, and averaging over the coupling between wave functions, as we did in eq 3b using eq 4b,

$$V = \kappa_{DA}|\sum_m \lambda_m \vec{u}_m||\sum_n \lambda_n \vec{u}_n|/4\pi\epsilon_0 R_{DA}^3 \tag{4a}$$

$$V = \sum_{m,n} \lambda_m \lambda_n \kappa_{mn} |\vec{u}_m||\vec{u}_n|/4\pi\epsilon_0 r_{mn}^3 \tag{4b}$$
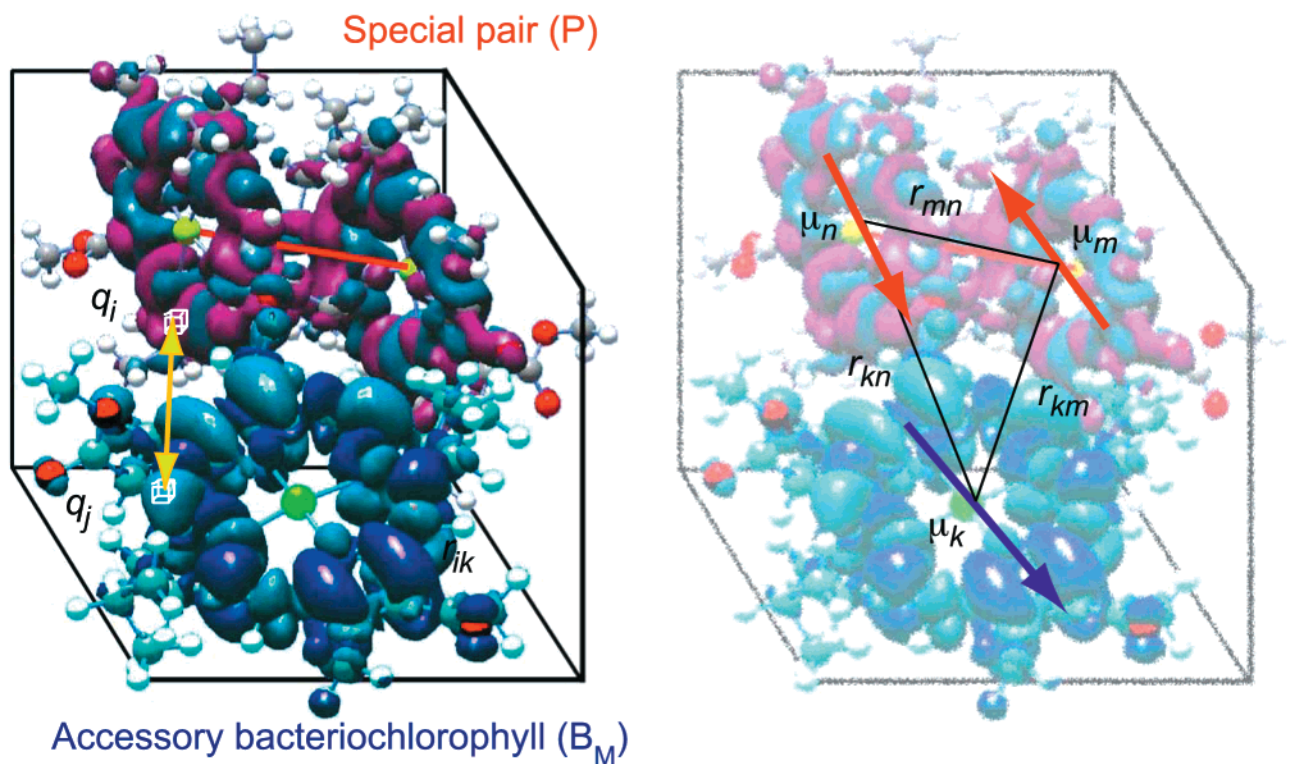
R_{DA} is the center-to-center separation between D and A and κ_{DA} is the orientation factor between $\vec{\mu}_D = \sum_m \lambda_m \vec{u}_m$ and $\vec{\mu}_A = \sum_n \lambda_n \vec{u}_n$. Transition dipoles μ_m and μ_n are separated by r_{mn} and oriented according to κ_{mn}. The coefficients λ_m and λ_n define the composition of wave functions D and A in terms of configurations m and n.

In a molecular aggregate we may consider the averaging of eqs 4a and 4b to be implemented on two levels. First, with respect to the coupling between sites.[21,25,27] This is the difference between partss a and b of Figure 3, which depicts the special pair and one accessory bacteriochlorophyll of the photosynthetic RC of a purple bacterium[33] (cf. Figure 1b). Part a of Figure 3 depicts an essentially exact calculation of the Coulombic coupling between a monomeric bacteriochlorophyll molecule k and the upper exciton state of a dimer formed by molecules m and n. This is accomplished by performing separate quantum chemical calculations of the ground and relevant excited states of k and the $m-n$ dimer in order to obtain the corresponding transition densities, $P_{0\delta}^k(\mathbf{r}_1)$ and $P_{\alpha 0}^{m-n}(\mathbf{r}_2)$ respectively, (which are plotted in the figure). These transition densities interact via the Coulomb potential to give the Coulombic interaction, eq 5, as described elsewhere,[27]

$$V^{Coul} = \frac{e^2}{4\pi\epsilon_0} \int \frac{P_{0\delta}^k(\mathbf{r}_1)P_{\alpha 0}^{m-n}(\mathbf{r}_2)}{|\mathbf{r}_1 - \mathbf{r}_2|} d\mathbf{r}_1 d\mathbf{r}_2 \tag{5}$$
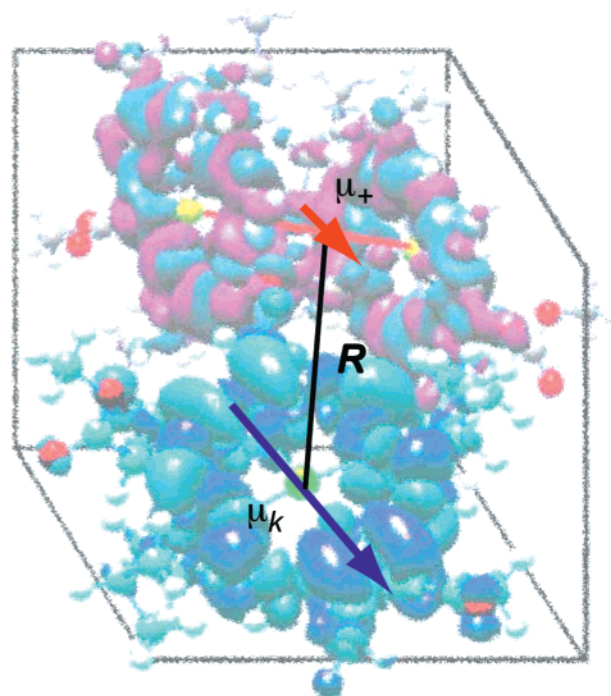
Figure 3b depicts a simplification of this method, which we see as the minimal representation of this aggregate.[28,29] Here the transition densities have been reduced to transition dipoles on each molecular center. For the monomer k we simply apply the dipole operator to the transition density $\mu_\zeta^{0\delta} = \int (r\zeta)_1 P_{0\delta}^k(\mathbf{r}_1)d\mathbf{r}_1$ (where ζ denotes the components of the vector). For the dimer, we need to ascertain the coefficients describing the admixture of monomer wave functions that comprise the dimer wave function, λ_m and λ_n. Then we can write $\mu_\zeta^{\alpha 0} = \lambda_m \mu_\zeta^{m0} + \lambda_n \mu_\zeta^{n0}$. We can then use eq 4b to determine the coupling.

Second, an averaging can be implemented with respect to the coupling within the donor or acceptor supermolecules, part c of Figure 3. In this case we would couple $\mu_\zeta^{0\delta}$ and $\mu_\zeta^{\alpha 0}$ directly, eq 4a. Such an averaging is invoked in analyses of RC energy transfer when, for example, either the P_- or P_+ special pair states are taken to be the energy acceptor in the Förster model, where donors and acceptors are treated as point dipoles associated with each spectroscopic band (i.e., P_+ and P_-). This approach fails to account for the true interactions within a multichromophoric assembly because length scales determining the couplings within the aggregate cannot be resolved by an optical spectrum because the wavelength of light used to measure such a spectrum is much greater than the interchromophore separations.

Förster Theory of Energy Transfer

J. Phys. Chem. B, Vol. 105, No. 8, 2001 **1643**

(a) Transition density cube (TDC) method.

(b) Distributed transition dipoles.

(c) Dipole approximation.

Figure 3. An illustration of three different schemes for calculating the electronic coupling between a monomeric donor B_M and the dimer P. (a) Couplings can be calculated from transition densities calculated for B_M and each of the exciton states of P. (b) This information can be reduced to dipole−dipole couplings between the B_M transition dipole moment and linear combinations of the P_L and P_M transition dipole moments. We suggest that this is the minimal acceptable representation of such an aggregate. (c) The exciton states of P can be further reduced to corresponding point dipoles. This corresponds to the Förster method.

We will summarize this section by stating that EET in a molecular aggregate proceeds not via molecular units nor collective emission/absorption spectra, but via electronic states. Thus, if there are m molecules that together make up the donor and n molecules that comprise the acceptor, then the EET dynamics must be determined by $m \times n$ electronic couplings. Owing to the distinct way that each electronic excited state is composed of the molecular wave functions, these $m \times n$ couplings will generally differ from one another. This is the role played by the λ_m and λ_n of eq 4. A general theory for the rate of EET in a molecular aggregate must explicitly account for each of these electronic couplings.

B. Definition of Donors and Acceptors. In a complex molecular aggregate the properties of the donor or acceptor will be modified if there are strong electronic interactions between the molecules that comprise D or A, respectively. Such interactions are manifest as perturbations to the D or A electronic spectra relative to those of the individual molecules. Both the electronic coupling factors and the spectral overlap factors associated with D and A will be consequently modified. We first simplify the problem by differentiating those interactions between the donor chromophores, between the acceptor chromphores, and the donor−acceptor interactions, as described with respect to Figure 1a.

For the general treatment of a set of donors and acceptors in close proximity we need to write a rate expression that satisfies the following criteria: (i) The couplings among the donors and among acceptors, V_{DmDn} and V_{AiAj} respectively, can take any values. This would range from "very weak", in which case the problem is reduced to pairwise energy transfer, to "strong", in which case the donor/acceptor absorption spectra differ significantly from those of the corresponding monomers. (ii) Static disorder, which affects both site energies and couplings, is properly accounted for (see section C). (iii) We want to retain, as far as possible, the "Förster-type" approach; that is, information regarding the donors and acceptors should be obtained from spectroscopic measurements. We note that by retaining the basic Förster approach, we must assume that the electronic states are linearly coupled to the phonon bath and that there is no correlation between the electron−phonon coupling amplitudes of the donor and acceptor states; hence, there are no coherence, or memory, effects.[23,34−36]

It is important that the coupling between D and A, V_{DmAj}, is classified as 'weak' so that, in accord with Förster theory, we can base our theory on the Fermi Golden Rule rate expression. This is tantamount to imposing a sequence of events in order of increasing time scales: (1) donor−donor and acceptor−acceptor electronic coupling, (2) homogeneous line broadening, (3) EET, (4) inhomogeneous line broadening. The conditions under which the FGR applies for energy transfer rate calculations have been examined many times.[37−40]

We begin by considering the full electronic Hamiltonian for the aggregate, in the spirit of the "multimer" model for electron-transfer introduced by Durrant et al.[41] Diagonalization of the complete Hamiltonian matrix results in electronic eigenstates that are orthogonal, and are of course uncoupled. Suitable donor and acceptor electronic states must be established as sets of electronically coupled donor and acceptor nonstationary states that we denote δ and α, respectively. This can be accomplished by partitioning the secular equations in the manner described by Löwdin.[42,43] We begin with the full set of secular equations for the system,

$$\sum_n (H_{nm} - \epsilon S_{nm})\lambda_n = 0 \qquad (6)$$

where λ_n are the eigenvectors and S_{mn} are the overlap matrix elements, usually taken to be $S_{mn} = \delta_{mn}$, where δ_{mn} is the kronecker delta. The diagonal Hamiltonian matrix elements $H_{nn} = E_n + \delta_n$ represent the electronic transition energies E_n of each molecule m, unperturbed by the other molecules, plus an energetic offset δ_n due to static disorder at this site.[44] This offset to the site energy arises owing to coupling between the molecule and slow motions in the surrounding environment. The off-diagonal Hamiltonian matrix elements $H_{mn} = V_{mn} + \delta_{mn}$ represent the electronic couplings between each pair of molecules m and n, V_{mn}, plus an optional offset due to off-diagonal disorder. We set $\delta_{mn} = 0$ here and in the following paper, however in a system in which the molecules have rotational degrees of freedom, for example, suitable distributions of pairwise couplings may need to be considered. This has been described by Marguet et al.[45] with reference to electronic interactions in columnar liquid crystals.

At this point we should introduce the effect of the medium with respect to dielectric screening of the electronic couplings between and among donors and acceptors in the Hamiltonian of eq 6. For a molecular aggregate, the dielectric screening must be incorporated at the level of the individual intersite couplings V_{DmDn}, V_{AiAj} and V_{DmAj}. Each coupling V is multiplied by the screening factor D.[30] Thus, it cannot be simply incorporated in the final rate expression as can be done for a two-molecule donor−acceptor system. Usually dielectric screening is assumed to have the form $D = n^{-2}$, where $n = \epsilon_R^{1/2}$ is the refractive index of the medium at optical frequencies. This limiting expression for D is appropriate only when V is a dipole−dipole coupling and the two chromophores are separated by a distance large compared to their sizes in a nondispersive, isotropic host medium, and local field corrections are negligible.[46] If these conditions hold, then it is likely that the theory we present here is unnecessary because the system cannot be a confined molecular aggregate.

In general we suggest that the corrections introduced by the dielectric medium will be fairly small, though certain specific interactions, for example, in a protein host, may be significant. A model for medium effects on closely spaced molecules has been developed recently in our laboratory. Hsu et al.[47] have suggested that for molecules that are distant from one another we can enclose each in a cavity such that the two cavities are separated by the dielectric medium. Solution of this model leads essentially to the result $D = n^{-2}$. However, when the molecules are closely spaced relative to their sizes, we need to reconsider such a treatment. Hsu et al. enclosed the pair of molecules in a cavity. They then found that the electronic coupling could be either decreased or increased, depending upon the orientation of the molecules and their positions within the cavity. In any case, because the dielectric medium is now confined to the outside of the cavity containing the dimer, the screening is smaller than for the case of well-separated molecules.

The secular eqs 6 can be partitioned into a matrix containing donor, acceptor and "bridge" blocks, eq 7,

$$\mathbf{M} = \begin{pmatrix} \mathbf{M}_{dd} & \mathbf{M}_{da} & \mathbf{M}_{db} \\ \mathbf{M}_{ad} & \mathbf{M}_{aa} & \mathbf{M}_{ab} \\ \mathbf{M}_{bd} & \mathbf{M}_{ba} & \mathbf{M}_{bb} \end{pmatrix} \qquad (7)$$

where we have used Löwdin's condensed notation: $\mathbf{M}_{mn} = H_{mn} - \epsilon S_{mn}$. Here "bridge" denotes any other configurations, such as connecting bonds, that can mediate superexchange coupling pathways. The partitioning of the Hamiltonian into donor $\mathbf{H}_d$ and acceptor $\mathbf{H}_a$ blocks is not always straightforward. One general recipe for the "optical partitioning" of the Hamil-

Förster Theory of Energy Transfer

J. Phys. Chem. B, Vol. 105, No. 8, 2001 **1645**

tonian is outlined as follows: (1) preparation of the system by a short optical pulse, (2) population relaxation and dephasing leads to a thermalized (or semithermalized) initial donor population, (3) this population can be used to define the {d}, (4) now {a} is defined as the set of molecules complementary to {d}. This type of protocol will be reliable provided that there is a separation of time scales between steps 1−3 and the time scale for the EET "hop" from donor to acceptor. More sophisticated models are necessary when the separation of time scales is in doubt, as have been considered previously.[23,35,36,48−50]

Now we find secular equations for the donor and acceptor blocks to be given by eqs 8,

$$(\mathbf{M}_{dd} - \mathbf{M}_{db}\mathbf{M}_{bb}^{-1}\mathbf{M}_{bd})\lambda_d = 0$$

$$(\mathbf{M}_{aa} - \mathbf{M}_{ab}\mathbf{M}_{bb}^{-1}\mathbf{M}_{ba})\lambda_a = 0 \qquad (8)$$

which leads to construction of the effective Hamiltonian of eq 9 in terms of the effective donor states δ and effective acceptor states α,

$$\mathbf{M} = \begin{pmatrix} \mathbf{M}_{\delta\delta} & \mathbf{M}_{\delta\alpha} \\ \mathbf{M}_{\alpha\delta} & \mathbf{M}_{\alpha\alpha} \end{pmatrix} \qquad (9)$$

The effective couplings are given by eq 10:

$$\mathbf{M}_{\delta\alpha} = \mathbf{M}_{da} - \mathbf{M}_{db}\mathbf{M}_{bb}^{-1}\mathbf{M}_{ba} \qquad (10)$$

Hence, diagonalization of the effective donor and effective acceptor Hamiltonians provides the sets of coefficients λ_d and λ_a, which defines the set of effective donor states $\Psi_\delta = \sum_{m\neq(\alpha)}\lambda_{\delta,m}\psi_m$, and the set of effective acceptor states $\Psi_\alpha = \sum_{n\neq(d)}\lambda_{\alpha,n}\psi_n$ in terms of linear combinations of site configurations. The Ψ_δ and Ψ_α are nonorthogonal, and yield the effective electronic couplings that promote the EET transition, eq 11

$$V_{\delta\alpha} = \langle\Psi_\alpha|V|\Psi_\delta\rangle = \sum_{m\neq(a)}\sum_{n\neq(d)}\lambda_{\delta,m}\lambda_{\alpha,n}V_{mn} \qquad (11)$$

A well-known manifestation of eq 11 is a superexchange-type electronic coupling factor. For example, we can consider a single donor d, an acceptor a and a bridge state b. The donor and acceptor wave functions assume the simple form

$$\Psi_\delta = N_\delta(\psi_d + \lambda_b\psi_b)$$

$$\Psi_\alpha = N_\alpha(\psi_a + \mu_b\psi_b) \qquad (12)$$

If we assume that the normalization factors $N_\delta \approx N_\alpha \approx 1$ (thus we have no interchromophore orbital overlap), and further assume that the mixing coefficients λ and μ are small (because b is a virtual state), then the donor−acceptor coupling is written,

$$V_{\delta\alpha} = \langle\Psi_\alpha|V|\Psi_\delta\rangle = V_{da} + \mu_b V_{db} + \lambda_b V_{ba} + \lambda_b\mu_b V_{bb} \simeq$$

$$V_{da} - \frac{V_{db}V_{ba}}{A_{ba}} - \frac{V_{db}V_{ba}}{A_{bd}} + \frac{V_{db}V_{bb}V_{ba}}{A_{ba}A_{bd}} \qquad (13)$$

where $A_{mn} = E_n - E_m$ and $V_{bb} = A_{ba}$. Thus, under weak coupling conditions, the interaction between our donor and acceptor states reduces to the perturbation theory expression familiar from treatments of superexchange interactions,[51] $V_{\delta\alpha} \approx V_{da} - V_{db}V_{ba}/A_{ba}$. Our calculations make no assumptions regarding the form of λ and μ.

C. Energetic Disorder and Ensemble Averaging. By definition, the line shapes $f^{hom}(\epsilon)$ and $a^{hom}(\epsilon)$ are identical for

all donors and acceptors, respectively. However, in many types of condensed phase media (e.g., glasses, crystals, proteins, surfaces), each of the donors and acceptors lie in a different local environment, which leads to a static offset of the excitation energy relative to the average, which persists longer than the time scale for EET. In such a case the measured donor emission and acceptor absorption spectra will not be representative of $f^{hom}(\epsilon)$ and $a^{hom}(\epsilon)$. When such "inhomogeneous" contributions to the line broadening become significant Förster theory cannot be used in an unmodified form.[30,52−56]

If there is just a single donor−acceptor pair, then we must ensemble average the nuclear spectral overlap. For example, if the inhomogeneous line broadening present in the donor emission spectrum $F(\epsilon)$ and acceptor absorption spectrum $A(\epsilon)$ is described by a function $G(\epsilon_m^0,\epsilon_m)$, which provides a distribution (often taken to be Gaussian) of static offsets ϵ_m to the mean excitation energy ϵ_m^0, then $F(\epsilon)$ and $A(\epsilon)$ are given by eqs 14a and 14b. These donor emission and acceptor absorption spectra are both, individually, ensemble average quantities and so are not related in a simple way to the spectral overlap, eq 14c:

$$F(\epsilon) = \int f^{hom}(\epsilon_d - \epsilon)G(\epsilon_d^0 - \epsilon_d)d\epsilon_d \qquad (14a)$$

$$A(\epsilon) = \int a^{hom}(\epsilon_a - \epsilon)G(\epsilon_a^0 - \epsilon_d)d\epsilon_a \qquad (14b)$$

$$J(\epsilon) = \int\int f^{hom}(\epsilon_d - \epsilon)G(\epsilon_d^0 - \epsilon_d)a^{hom}(\epsilon_a - \epsilon) \times$$
$$G(\epsilon_a^0 - \epsilon_a)d\epsilon_d d\epsilon_a \qquad (14c)$$

In the present work, we need to accommodate coupling among the donor and/or acceptor chromophores, especially coupling that perturbs the donor emission or acceptor absorption spectrum. For such a molecular aggregate, the site energy disorder affects both the electronic and the nuclear factors simultaneously. We have described already that if there are m molecules that together make up the donor and n molecules that comprise the acceptor, then the EET dynamics must be determined by $m \times n$ electronic couplings. So to introduce disorder properly into the EET rate calculation, each of the $m \times n$ electronic couplings $V_{\delta\alpha}$ must be associated with a corresponding spectral overlap factor $J_{\delta\alpha}(\epsilon)$.[30] This provides us with the *dimensionless* coupling-weighted spectral overlap for each interaction, $u_{\delta\alpha}(\epsilon) = |V_{\delta\alpha}|^2 J_{\delta\alpha}(\epsilon)$. This quantity governs the mechanism by which EET is promoted in complex aggregates. For example, we can ascertain which electronic states most significantly mediate the EET by comparing the values of each of the $\int d\epsilon u_{\delta\alpha}(\epsilon)$, which are directly proportional to the rate for each pathway.

We incorporate disorder into the calculation by ensemble-averaging the set of coupling-weighted spectral overlaps for many aggregates using a Monte Carlo method. In this way the effect of disorder on both electronic couplings and spectral overlap is accounted for by ensemble averaging $\sum_{\delta,\alpha}u_{\delta\alpha}(\epsilon)$. Note that we assume that the homogeneous spectral line shapes are independent of disorder except for an origin shift.

In Figure 4 we consider an example of EET from an essentially monomeric donor, a single B800 bacteriochlorophyll molecule, to a complex acceptor, the B850 ring of LH2, which consists of 18 coupled bacteriochlorophyll chromophores.[1,2,57] In this case the nearest-neighbor electronic couplings between the acceptor molecules are of the order of 300 cm^{-1} and the disorder is $\sigma = 160$ cm^{-1}. The absorption spectrum of this B850 ring exhibits an intense peak at 865 nm and a series of states with very little oscillator strength throughout the region from
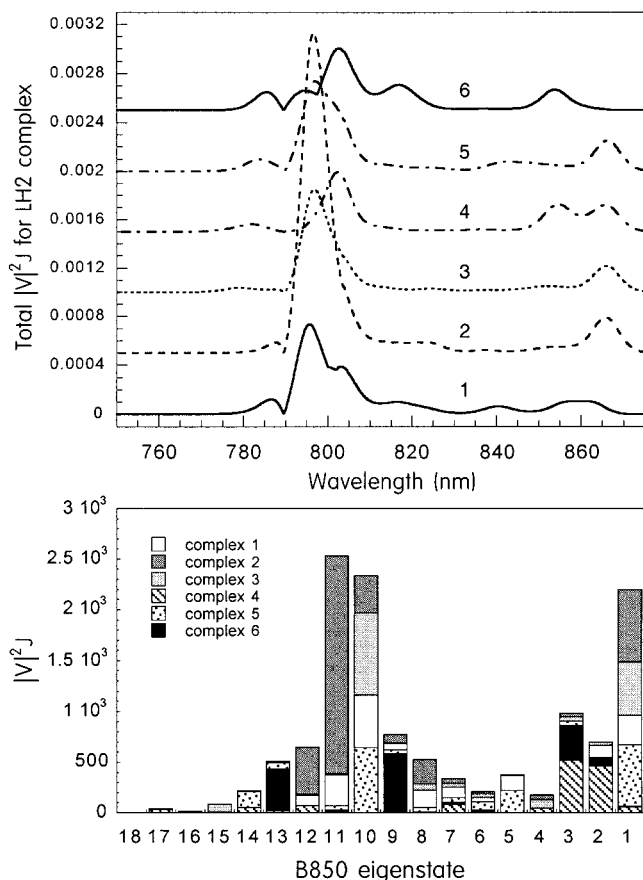
Figure 4. Calculations of the EET from B800 to B850 in the peripheral light harvesting complex LH2 of the purple bacterium *Rb. sphaeroides*. (a) In the upper part we plot the calculated $\sum_\alpha |V_{B800-\alpha}|^2 J_{B800-\alpha}(\epsilon)$ (i.e., summed over all 18 of the B850 acceptor states α) for six individual LH2 complexes taken at random from the ensemble. The differences between each of these contributions to the ensemble average EET rate are due to the effect of static disorder on electronic couplings and spectral overlaps. (b) In the lower part we show a histogram which indicates the contribution to the total ensemble average rate of $\int d\epsilon \sum_\alpha |V_{B800-\alpha}|^2 J_{B800-\alpha}(\epsilon)$ from each B850 eigenstate α, numbered 1–18 along the abcissa, of each of the six LH2 complexes. There is an approximate correspondence between the abcissae of the upper and lower plots (i.e., eigenstates 10–11 have eigenvalues in the range ~790–800 nm).

850 to 750 nm. The emission maximum of the B800 donor is at approximately 800 nm. In Figure 4a we show the $|V|^2 J(\epsilon)$ calculated for B800 → B850 EET within six individual LH2 complexes, summed over all 18 of the B850 acceptor eigenstates. Inspection of the $|V|^2 J(\epsilon)$ plots reveals that disorder is partly responsible for introducing coupling between the B800 donor bacteriochlorophyll and the "dark" exciton states of B850. Thus, energy flows from the B800 ring to the upper exciton manifold of B850, rather than directly to the bright B850 absorption band at 865 nm. This mechanism of energy flow is not suggested in any way by inspection of the acceptor absorption spectrum.

Disorder plays an important role in determining the observed EET rate for this system. It provides a uniform, temperature-independent acceptor density of states, which in turn leads to the observed temperature-independence of EET in this system. An inspection of the six $|V|^2 J(\epsilon)$ plots indicates that, owing to disorder, energy flow in each LH2 complex is quite unique. In Figure 4b we dissect this analysis further. We show how each eigenstate of each of the six individual LH2 complexes contributes to the ensemble average $|V|^2 J(\epsilon)$, and hence the rate

of B800 → B850 EET. We can see that the principle acceptor states of B850 are the eigenstates 1−3 and 8−13, which correspond to the peaks in the $|V|^2 J(\epsilon)$ plot, Figure 4a, centered at ~860 and ~800 nm, respectively. It is evident that the contribution to the total B800 → B850 rate from each B850 acceptor eigenstate is very sensitive to disorder because the bars making up the histogram vary in size dramatically from one complex to another.

D. Calculation of the EET Rate for Molecular Aggregates. Now that we have examined the key components that must be incorporated into a theory for EET in molecular aggregates, we will bring everything together into a general rate expression. Underpinning our approach are (i) explicit separation of electronic and nuclear factors in the rate expression; (ii) calculation of the effective electronic couplings using the basis set of the molecules that comprise the aggregate, (iii) Careful calculation of the nuclear spectral overlap factors; (iv) the association of each coupling $V_{\delta\alpha}$ with a corresponding spectral overlap factor $J_{\delta\alpha}(\epsilon)$ in order to generate the dimensionless coupling-weighted spectral overlap for each interaction, $u_{\delta\alpha}(\epsilon) = |V_{\delta\alpha}|^2 J_{\delta\alpha}(\epsilon)$; and (v) taking an ensemble average over many aggregates. Under the assumption of weak coupling between donors and acceptors (but not *among* either donors or acceptors), an expression for the rate of energy transfer from donor states δ to acceptor states α that incorporates all these concepts is given by eq 15,

$$k = \frac{2\pi}{h} \left\langle \int_0^\infty d\epsilon \sum_{\delta,\alpha} P_\delta |V_{\delta\alpha}(\epsilon_d,\epsilon_a)|^2 J_{\delta\alpha}(\epsilon,\epsilon_d,\epsilon_a) \right\rangle_{\epsilon_d,\epsilon_a} \quad (15)$$

where $V_{\delta\alpha}$ are the electronic couplings between the effective donors and acceptors, as described in section II.B, and ϵ_d and ϵ_a represent static offsets from the mean of the donor and acceptor excitation energies as described in the previous section. Thus, it is emphasized that both the couplings and the spectral overlaps depend on disorder. It is assumed that each $V_{\delta\alpha}(\epsilon_d,\epsilon_a)$ does not vary across the energy spectrum of its corresponding $J_{\delta\alpha}(\epsilon,\epsilon_d,\epsilon_a)$. P_δ is a normalized Boltzmann weighting factor for the contribution of δ to the thermalized donor state, $P_\delta = \exp[(\epsilon_{\delta=1} - \epsilon_\delta)/kT]/\sum_\delta \exp[(\epsilon_{\delta=1} - \epsilon_\delta)/kT]$. The angle brackets denote that an ensemble average is taken over many aggregate units (e.g., RC complexes) so as to account for static disorder in the monomer site energies. The spectral overlap between bands δ and α is defined in terms of donor and acceptor densities of states as in eq 16,

$$J_{\delta\alpha}(\epsilon,\epsilon_d,\epsilon_a) = N_\alpha a_\alpha^{\text{hom}}(\epsilon,\epsilon_d,\epsilon_a) N_\delta f_\delta^{\text{hom}}(\epsilon,\epsilon_d,\epsilon_a) \quad (16)$$

Note that each $J_{\delta\alpha}(\epsilon,\epsilon_d,\epsilon_a)$ is associated with an electronic coupling factor $V_{\delta\alpha}(\epsilon_d,\epsilon_a)$ within the ensemble average. The $f_\delta^{\text{hom}}(\epsilon,\epsilon_d,\epsilon_a)$ and $a_\alpha^{\text{hom}}(\epsilon,\epsilon_d,\epsilon_a)$ specify the donor and acceptor densities of states (D.O.S.), as described in the accompanying paper. The dependence upon disorder is assumed to introduce a static offset of the origin, as is usually assumed.[44] These D.O.S. represent the emission (absorption) line shape of the donor (acceptor), calculated without disorder (hence the superscript ′hom′) and without dipole strength. N_δ and N_α are area normalization constants such that $1/N_\delta = \int_0^\infty d\epsilon f_\delta^{\text{hom}}(\epsilon,\epsilon_d,\epsilon_a)$ and $1/N_\alpha = \int_0^\infty d\epsilon a_\alpha^{\text{hom}}(\epsilon,\epsilon_d,\epsilon_a)$.

Our procedure requires as input a site representation of the electronic Hamiltonian which we can modify by adding disorder to the site energies. Using this 'disordered' Hamiltonian, we find the set of effective donor states δ, effective acceptor states α, and the couplings between them $V_{\delta\alpha}(\epsilon_d,\epsilon_a)$. We can

Förster Theory of Energy Transfer

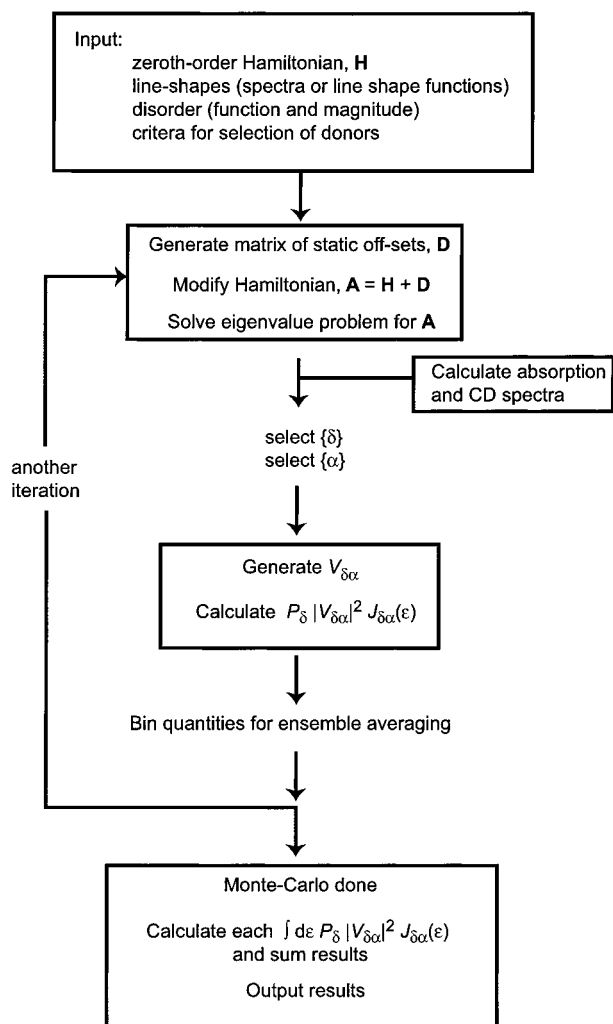*J. Phys. Chem. B, Vol. 105, No. 8, 2001* **1647**

Figure 5. A flowchart illustrating our computational procedure for calculating EET rates using eq 15.

think of the $\{\delta\}$ as collectively comprising the donor emission spectrum, and the $\{\alpha\}$ as collectively comprising the acceptor absorption spectrum. For each δ and α we wish to calculate $|V_{\delta\alpha}(\epsilon_d,\epsilon_a)|^2 J_{\delta\alpha}(\epsilon,\epsilon_d,\epsilon_a)$, the dimensionless quantity that defines the rate of $\delta\rightarrow\alpha$ EET. For this strategy to work, the $V_{\delta\alpha}$ must be classified as "weak". To determine $J_{\delta\alpha}(\epsilon_d,\epsilon_a)$ we need electron–phonon coupling information together with intramolecular vibrational information in terms of a line shape function or spectral density that relates to the eigenstate representation. We can input this information using explicit equations, as we do in the companion paper,[31] but since the line shape information is contained in experimental emission and absorption spectra (in the absence of significant inhomogeneous line broadening), experimental spectra may also be used in many cases.[58]

The important points pertaining to eq 15 are the following: (a) it accounts explicitly for electronic couplings between all possible δ/α pairs and weights each of these couplings $V_{\delta\alpha}$ with an associated nuclear spectral overlap factor $J_{\delta\alpha}$, and (b) an ensemble average over disorder is taken at the level of the site energies. In an aggregate, disorder affects both $V_{\delta\alpha}$ (via the coefficients $\lambda_{\delta,n}$ and $\lambda_{\alpha,m}$) and $J_{\delta\alpha}$. Our procedure to calculate EET rates is summarized in Figure 5.

III. Implementing the Theory

The origin of the electronic coupling factors V_{mn} determines the mechanism of the energy transfer. For example, if V_{mn} is

dominated by the Coulombic coupling between electronic transition moments of monomeric donor site m and monomeric acceptor site n, V_{mn}^{Coul}, then the energy transfer rate will often exhibit a characteristic R^{-6} distance dependence. It is known that this is usually the case when the intermolecular separation R is large compared to the sizes of the molecules and the electronic transitions of donor m and acceptor n are electric dipole-allowed. The photosynthetic reaction center,[33] Figure 1b, is an example of a system in which the donor and acceptor molecules are closely spaced relative to their molecular dimensions. For example, the BChl molecule is 17 Å across, while the distance between ring centers are as follows: 7.0 Å between P_L and P_M, 10.4 Å between P_L and B_L, and 10.2 Å between B_L and H_L. The distance of closest contact between the chromophore pairs listed above are 2.2, 2.6, and 3.3 Å. The close proximity between chromophores in the RC means that a range of distances determine inter-chromophore interactions. In turn, for the electronic interactions to be determined accurately, they should be calculated according to eq 5 because any "pre-averaging" such as a multipolar expansion of the interaction potential will be poorly convergent.

For example, in Figure 6 we compare transition densities calculated for the special pair upper exciton state P_+ (upper part) and lower exciton state P_- (lower part). The P_+ transition density has many alternating positive and negative phase regions that are averaged away by the dipole operator to give a small transition dipole moment. The P_- transition density has one region of negative phase and another region of positive phase, indicative of a dipole allowed transition, that are averaged by the dipole operator to give a large transition dipole moment. Such an averaging over the topology of the transition density is carried out by light, which has a wavelength large compared to molecular dimensions and separations, and is therefore manifest in the absorption and emission spectra. Thus, according to Förster theory the electronic coupling between donor B_M and acceptor P_+ is determined according to reduced model shown in Figure 3c. The minimal model that encompasses the molecular composition of the aggregate is the model depicted in Figure 3b and is calculated using eq 4b.

As we have already stressed, it is not possible to use the spectroscopic band alone to estimate donor–acceptor coupling in the manner advocated by Förster. In a molecular aggregate, the δ-α couplings tend to be linear combinations of couplings between the individual molecules that comprise the aggregate. For the RC, the couplings derive from the full 6×6 Hamiltonian that includes all molecules in the aggregate (P_M, P_L, B_M, B_L, H_M, and H_L), and the electronic couplings between them (e.g., (B_M–P_L)) as determined by their arrangement (i.e., atomic centers of the X-ray crystal structure). We reiterate that the δ–α couplings are not revealed in a simple way by the spectroscopic bands.

Löwdin partitioning of the full RC Hamiltonian for B to P EET yields a reduced Hamiltonian for the donor involving the Bs and Hs, while the corresponding reduced acceptor Hamiltonian involves the Ps and Hs, as shown schematically in Figure 7. Partitioning the system Hamiltonian into donor, acceptor and bridge blocks can be achieved numerically, based on calculated absorption spectra of molecules within the ensemble of aggregates, beginning with the optical preparation of the donor state. In the case of the RC, this leads to optical preparation of either B_L or B_M because they have large oscillator strengths at 800 nm. It is possible to excite one or other preferentially depending on the excitation wavelength, but we do not consider this here. In practice, we partition the Hamil-
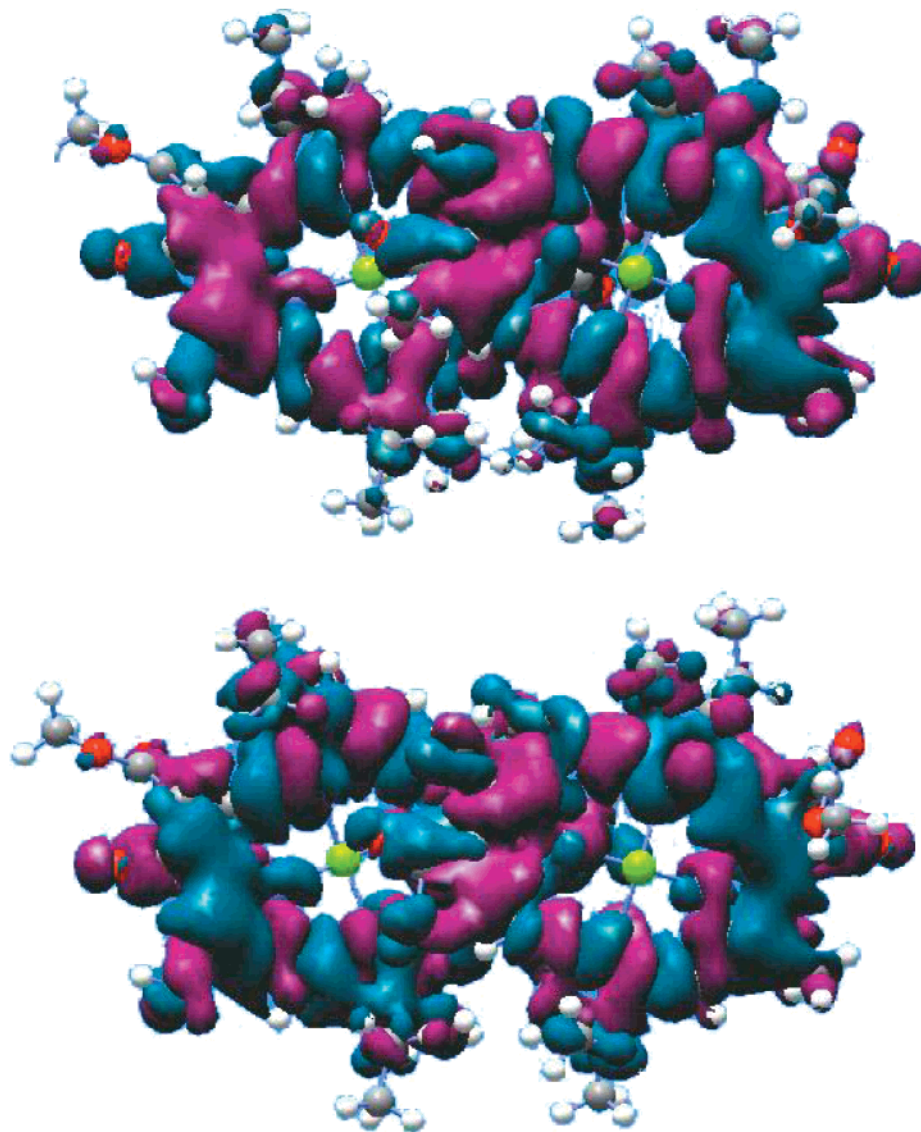
Figure 6. Transition densities calculated for the special pair (CIS/3-21G*). (a) Upper part, P– state, and (b) lower part, the P+ state.

tonian for B to P EET by looking for those eigenstates with large *B* coefficients (effective donor eigenstates) and those with large *P* coefficients (effective acceptor eigenstates).

When energy transfer from B to P is calculated, H merely mixes electronically with both Bs when partitioning the reduced donor Hamiltonian and with the Ps when partitioning the reduced acceptor matrix. Solving these reduced secular equations yields a set of four donor states Ψ_δ and a set of four acceptor states Ψ_α in terms of linear combinations of all the RC pigment molecules ψ_n. Of these four donor states, we retain the two that have the largest coefficients $\lambda_{\delta,m}$ of the monomer sites where $m = B_L$ and B_M, and label them B– ($\delta = 1$ of Figure 7) and B+ ($\delta = 2$ of Figure 7). Similarly, of the four possible acceptor states, the two with the largest coefficients of the monomer acceptor sites $\lambda_{\alpha,n}$ where $n = P_L$ and P_M are assigned to the lower energy acceptor state P– ($\alpha = 1$ of Figure 7) and the higher energy acceptor state P+ ($\alpha = 2$ in Figure 7). The δ and α states that we disregard are the complementary states, composed mostly of H_M and H_L. Obviously these are not primary donor or acceptor states because they are too high in energy. We could still include them in our calculation if we wished, but would find that the complementary donor states are excluded via the P_δ distribution factor, and the comple-

mentary acceptors would be rendered superfluous by their negligibly small spectral overlaps with the donors.

In a similar manner as described above, the theory can be applied to assign donor and acceptor states in the energy transfer pathway from H to B. In this case, the two reduced Hamiltonians are different from those shown in Figure 7. In the energy transfer step from H to B, P can act as a bridge to allow electronic mixing with both H and B because the reduced donor Hamiltonian contains the nonzero electronic coupling matrix elements between H and P monomers, while the reduced acceptor Hamiltonian only has nonzero coupling matrix elements between the B and P monomers. This is important because the $B_M–P–B_L$ coupling pathways are more significant than the direct $B_M–B_L$ coupling. After solving the reduced secular equations, the donor states, H_+ and H_- and the acceptor states, B_+ and B_- are obtained.

IV. Discussion

We have described in this paper how the ideas reported over 50 years ago by Förster can be applied to model EET dynamics in complex aggregates in which interactions involving more than just one donor and acceptor are significant. In any system where
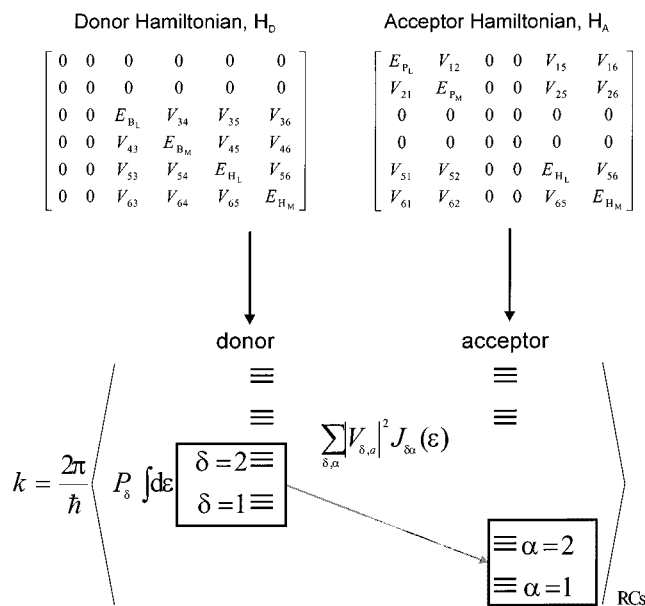
Förster Theory of Energy Transfer

J. Phys. Chem. B, Vol. 105, No. 8, 2001 **1649**

Donor Hamiltonian, H_D

$$\begin{bmatrix} 0 & 0 & 0 & 0 & 0 & 0 \\ 0 & 0 & 0 & 0 & 0 & 0 \\ 0 & 0 & E_{B_L} & V_{34} & V_{35} & V_{36} \\ 0 & 0 & V_{43} & E_{B_M} & V_{45} & V_{46} \\ 0 & 0 & V_{53} & V_{54} & E_{H_L} & V_{56} \\ 0 & 0 & V_{63} & V_{64} & V_{65} & E_{H_M} \end{bmatrix}$$

Acceptor Hamiltonian, H_A

$$\begin{bmatrix} E_{P_L} & V_{12} & 0 & 0 & V_{15} & V_{16} \\ V_{21} & E_{P_M} & 0 & 0 & V_{25} & V_{26} \\ 0 & 0 & 0 & 0 & 0 & 0 \\ 0 & 0 & 0 & 0 & 0 & 0 \\ V_{51} & V_{52} & 0 & 0 & E_{H_L} & V_{56} \\ V_{61} & V_{62} & 0 & 0 & V_{65} & E_{H_M} \end{bmatrix}$$

donor   acceptor

$$k = \frac{2\pi}{\hbar} \; P_\delta \int d\varepsilon \; \sum_{\delta,a} |V_{\delta,a}|^2 J_{\delta a}(\varepsilon)$$

Figure 7. A schematic depiction of the partitioning of the RC Hamiltonian into donor and acceptor, enabling the calculation of the effective electronic couplings.

Figure 8. Results of calculations of the EET from B800 to B850 in the peripheral light harvesting complex LH2 of the purple bacterium *Rb. sphaeroides* for six individual LH2 complexes taken at random from the ensemble. We have plotted relative dipole strength calculated for each B850 eigenstate against the corresponding coupling to B800.

the electronic spectroscopy of a donor molecule or an acceptor molecule is perturbed by interactions with any other donors or acceptors respectively, our generalized Förster theory, eq 15, can be used to calculate EET dynamics.

The essential features of this equation are that, first, it divides the problem into EET pathways between a set of effective donors and effective acceptors. These effective donors and acceptors can be thought of as electronic transitions of individual donor/acceptor molecules that have been renormalized (or dressed) by electronic interactions with all other donor/acceptor molecules. This provides the basis set that we use to keep count of all the electronic states involved in the problem. Using this basis set for determining the electronic couplings between effective donors and acceptors introduces the concept that the electronic coupling factors must be calculated by considering the arrangement of the molecules, not by considering the electronic spectra, Figure 3.

The details of interactions within an aggregate of molecules cannot be satisfactorily resolved by spectra when the wavelength of light is much larger than molecular separations. Hence arguments that relate transition oscillator strength (or rather, transition dipole moment) to electronic couplings, and therefore energy transfer times, in molecular aggregates are incorrect. For example, consider Figure 8. Here we plot the relative dipole strength of each B850 eigenstate against the corresponding coupling to B800 for six individual *Rb. sphaeroides* LH2 complexes taken at random from the ensemble average calculations reported in ref 30. If there were a relationship between the transition dipole moment of the B850 acceptor transition and the electronic coupling between B800 and this transition, this would be evident as a correlation between these two quantities. This plot shows a striking absence of any correlation between B850 dipole strength and B800−B850 coupling. The reason for this is that the dipole strength of the B850 transition is an average property of the entire B850 ring, while the electronic coupling to the B800 molecule is determined mostly by just a small section of the B850 ring.

Each of the electronic couplings in eq 15 is associated with a corresponding spectral overlap factor. To calculate the spectral
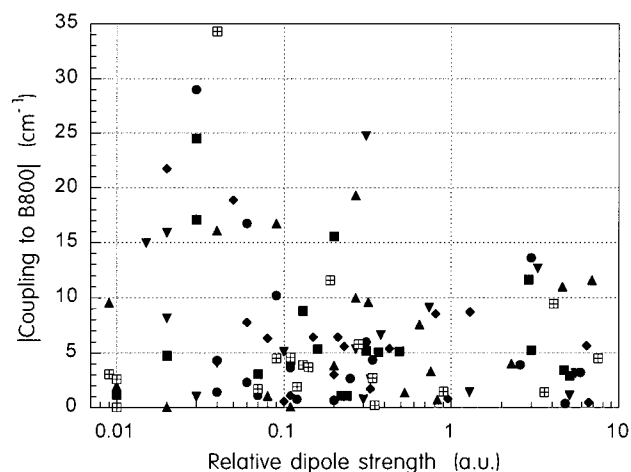
overlaps we add a dressing due to electron−phonon interactions to our effective donor and acceptor states. This dressing of the bare electronic transitions is seen as line broadening and vibronic progressions in the spectra. It provides the energy conservation conditions and density of final states, as described by Förster. In the present work we have not considered effects that may arise owing to entanglement of electronic coupling and electron−phonon-interactions. Such effects have been carefully considered previously,[34,35] and such work represents an important extension of Förster theory for the case of a single donor−acceptor pair. Jackson and Silbey,[34] for example, calculated the rate of EET between impurity centers in solids to infinite order in the donor/acceptor-phonon interaction. They obtained their result by calculating the interaction between "clothed" donor and acceptor states, which accounts for the lattice distortion about each molecule as a function of the molecule's electronic state. The degree of this distortion determines the extent of delocalization of the excitation. Introducing such features into our model would provide a powerful means for calculating EET dynamics in any aggregate without having to impose our time scale separation constraints. Our limiting model assumes that the electron−phonon interactions simply provide a smooth distribution of initial states and a final state quasicontinuum that ensures energy conservation and transition irreversibility. We note that this limit of the more sophisticated models has proven to be simple and effective; and does generally retrieve the correct physical picture for EET between large molecules.[30,31,58]

It is well-known that electron−phonon interactions tend to localize electronic states. It is such a concept that leads to eq 15 being able to extrapolate smoothly between cases where there are strong couplings among donors and/or acceptors, to that where those couplings are negligible; which is when Förster's equation applies. For example, resorting to the model of a single donor and two acceptors, Figure 2, we can demonstrate that eq 15 reduces to a sum of pairwise rates when the electronic coupling between the acceptor molecules X and Y is small compared to the width of their absorption bands. Equation 15 is written in terms of the mixed acceptor states $A_+ = \cos\theta|X^*Y\rangle + \sin\theta|XY^*\rangle$ and $A_- = \sin\theta|X^*Y\rangle - \cos\theta|XY^*\rangle$, for arbitrary coupling and site energies related by $\tan2\theta = 2V_{XY}/(E_X - E_Y)$. The two nuclear spectral overlap factors are $J_{DA+} \approx J_{DA-} = J$ because the exciton splitting and level shift caused by the electronic coupling are small

compared to the line width. So the total rate of energy transfer from D to A is

$$k = \frac{2\pi}{\hbar}|V_{\mathrm{DA+}}|^2 J_{\mathrm{DA+}} + \frac{2\pi}{\hbar}|V_{\mathrm{DA-}}|^2 J_{\mathrm{DA-}} = \frac{2\pi}{\hbar}(|V_{\mathrm{DX}}|^2 + |V_{\mathrm{DY}}|^2)J \quad (17)$$

where the electronic factors have been converted to the site representation and simplified using standard trigonometric relations. It is thus evident that the energy transfer rate reduces to a sum of pairwise rates when the couplings between donors and that between acceptors is smaller than the line width of their respective emission and absorption bands. In other words, the emission and absorption densities of states must look like those of a single donor and acceptor, respectively.

A last feature of eq 15 is that static disorder in the donor/acceptor site energies that arises from slow fluctuations of the environment is incorporated through ensemble averaging. This also has the effect of localizing donors and acceptors, and for large values of disorder eq 15 reduces to a Förster-type picture in a manner analogous to that illustrated above for electron−phonon coupling arising from fast fluctuations. In molecular aggregates site energy disorder affects both the spectral overlap and the nature of the effective donor and acceptor states, and hence the effective couplings.

We notice that eq 15 is a Fermi Golden Rule rate expression involving multiple initial-final state pathways. Use of the Fermi Golden Rule formalism is contingent upon physical irreversibility of the EET process. If the excitation does return to the donor from the acceptor, then there must be no "memory" affects, or coherence, associated with the previous donor−acceptor EET process. Such conditions are often realized in the condensed phase, where donor and acceptor electronic transitions interact with a dissipative system possessing an infinite number of degrees of freedom and continuous energy spectrum (the nuclear motions of the bath). Generally speaking, when electron−nuclear interactions are larger than the electronic couplings then one expects the Fermi Golden Rule to be a reasonable approximation. When the separation of time scales that we described in section II.B cannot be made, then the problem becomes quite complicated.[23,35,36,48−50] In the simplest case we might find that each *J* assumes a time dependence. Then the transition probability exhibits a time dependence. In more complex systems we can envisage that the definition of effective donors and acceptors changes with time. Kimura et al.[50] have examined 'non-Golden Rule' EET dynamics in detail recently.

V. Conclusions

In summary, our eq 15 converges to the Förster equation only when all the following points are satisfied: (a) the spatial distribution of donors and acceptors in the assembly is such that each of the donor−donor, donor−acceptor, and acceptor−acceptor interaction introduces a negligible perturbation to the absorption line shape; (b) the separation between donor and acceptor is large compared to the molecular dimensions; (c) optical transitions of donor and acceptor are strongly electric dipole allowed; and (d) energetic disorder is negligible. In the present work we have found that very weak or even normally forbidden transitions in a molecular aggregate may participate in efficient energy transfer via a Coulombic coupling mechanism, rather than an orbital overlap (e.g., electron exchange or Dexter) mechanism as is often supposed. It seems likely that the remarkably efficient energy transfer in various photosyn-

thetic pigment−protein complexes will be understandable in this context. A primary implication of this work is that the fundamental limitations of optical spectroscopy hinder its application to determine electronic couplings in molecular aggregates. This means that, at the present time, general design principles for light harvesting structures can only be revealed by a combination of experiment and theory. Finally, these ideas may open new possibilities in the design of synthetic EET devices.

References and Notes

(1) van Grondelle, R.; Dekker: J. P.; Gillbro, T.; Sundström, V. *Biochim. Biophys. Acta* **1994**, *1187*, 1−65.

(2) Sundström, V.; Pullerits, T.; van Grondelle, R. *J. Phys. Chem. B* **1999**, *103*, 2327.

(3) Guillet, J. E. *Polymer Photophysics and Photochemistry*; Cambridge University Press: Cambridge, 1985.

(4) Webber, S. E. *Chem. Rev.* **1990**, *90*, 1469−1482.

(5) Balzani, V.; Scandola, F. *Supramolecular Photochemistry*; Ellis Horwood: Chichester, 1991.

(6) Venturi, M.; Serroni, S.; Juris, A.; Campagna, S.; Balzani, V. *Top. Curr. Chem.* **1998**, *197*, 194−228.

(7) Jullien, L.; Canceill, J.; Valeur, B.; Bardez, E.; Lefevre, J.-P.; Lehn, J.-M.; Marchi-Artzner, V.; Pansu, R. *J. Am. Chem. Soc.* **1996**, *118*, 5432−5442.

(8) Kuciauskas, D.; Liddell, P. A.; Lin, S.; Johnson, T. E.; Weghorn, S. J.; Lindsay, J. S.; Moore, A. L.; Moore, T. A.; Gust, D. *J. Am. Chem. Soc.* **1999**, *121*, 8604−8614.

(9) van Patten, P. G.; Schreve, A. P.; Lindsey, J. S.; Donohoe, R. J. *J. Phys. Chem. B* **1998**, *102*, 4209−4216.

(10) Li, F.; Yang, S. I.; Ciringh, Y.; Seth, J.; Martin, C. H.; Singh, D. L.; Kim, D.; Birge, R. R.; Bocian, D. F.; Holten, D.; Lindsey, J. S. *J. Am. Chem. Soc.* **1998**, *120*, 10001−10017.

(11) Förster, T. *Ann. Phys.* **1948**, *6*, 55−75.

(12) Mukamel, S. *Principles of Nonlinear Optical Spectroscopy*; Oxford University Press: New York, 1995.

(13) Fleming, G. R.; Passino, S. A.; Nagasawa, Y. *Philos. Trans. R. Soc. London A* **1998**, *356*, 389−404.

(14) According to Förster, the rate of EET from donor D to acceptor A is given by

$$k^{\mathrm{Förster}} = \frac{1}{\tau_D}\frac{9000(\ln 10)\kappa^2\phi_D I(\bar{\nu})}{128\pi^5 Nn^4}\frac{1}{R^6}$$

where the symbols are defined elsewhere and the Förster spectral overlap is defined as

$$I(\bar{\nu}) = \int \frac{\bar{a}_A(\bar{\nu})\bar{f}_D(\bar{\nu})}{\bar{\nu}^4}d\bar{\nu}$$

This Förster spectral overlap integral is obtained from the overlap − on a wavenumber scale − of an experimentally measured absorption spectrum for A, with intensity in molar absorbance, with an area-normalized emission spectrum of D.

(15) Van der Meer, B. W.; Coker, G. I.; Chen, S.-Y. *Resonance Energy Transfer, Theory and Data*; VCH Publishers: New York, 1994.

(16) Lin, S. H. *Mol. Phys.* **1971**, *21*, 853−863.

(17) Berlman, I. B. *Energy Transfer Parameters of Aromatic Compounds*; Academic Press: New York, 1973.

(18) dos Remedios, C. G.; Moens, P. D. J. In *Resonance Energy Transfer*; Andrews, D. L., Demidov, A. A., Eds.; Wiley: Chichester, 1999; pp 1−64.

(19) Tollin, G.; Sogo, P. B.; Calvin, M. *Ann. N. Y. Acad. Sci.* **1958**, *74*, 310−328.

(20) Andrews, D. L. *Chem. Phys.* **1989**, *135*, 195−210.

(21) Dexter, D. L. *J. Chem. Phys.* **1953**, *21*, 836−850.

(22) Craig, D. P.; Walmsley, S. H. *Excitons in Molecular Crystals*; Benjamin: New York, 1968.

(23) Grover, M.; Silbey, R. *J. Chem. Phys.* **1971**, *54*, 4843−4851.

(24) London, F. *J. Phys. Chem.* **1942**, *46*, 305−316.

(25) Czikklely, V.; Forsterling, H. D.; Kuhn, H. *Chem. Phys. Lett.* **1970**, *6*, 207−210.

Förster Theory of Energy Transfer

J. Phys. Chem. B, Vol. 105, No. 8, 2001 **1651**

(26) Chang, J. C. *J. Chem. Phys.* **1977**, *67*, 3901−3909.

(27) Krueger, B. P.; Scholes, G. D.; Fleming, G. R. *J. Phys. Chem. B* **1998**, *102*, 5378−5386.

(28) Valkunas, L.; Kudzmauskas, S.; Juzeliunas, G. *Sov. Phys. Coll.* **1985**, *25*, 41−46.

(29) Sumi, H. *J. Phys. Chem. B* **1999**, *103*, 252−260.

(30) Scholes, G. D.; Fleming, G. R. *J. Phys. Chem. B* **2000**, *104*, 1854−1868.

(31) Jordanides, X. J.; Scholes, G. D.; Fleming, G. R. *J. Phys. Chem. B* **2001**, *105*, 1652.

(32) Scholes, G. D.; Andrews, D. L. *J. Chem. Phys.* **1997**, *107*, 5374−5384.

(33) Hoff, A. J.; Deisenhofer, J. *Phys. Rep.* **1997**, *287*, 1−247.

(34) Jackson, B.; Silbey, R. *J. Chem. Phys.* **1983**, *78*, 4193−4196.

(35) Soules, T. F.; Duke, C. B. *Phys. Rev. B* **1971**, *3*, 262−274.

(36) Kenkre, V. M. *Phys. Rev. B* **1975**, *12*, 2150−2160.

(37) Robinson, G. W.; Frosch, R. P. *J. Chem. Phys.* **1962**, *37*, 1962−1973.

(38) Dexter, D. L.; Förster, T.; Knox, R. S. *Phys. Status. Solidi.* **1969**, *34*, K159−K162.

(39) Agabekyan, A. S.; Melikyan, A. O. *Opt. Spectrosc.* **1972**, *32*, 153−157.

(40) Burshtein, K. Y.; Kozhushner, M. A. *Sov. Phys.−Solid State* **1971**, *13*, 404−409.

(41) Durrant, J. R.; Klug, D. R.; Kwa, S. L. S.; van Grondelle, R.; Porter, G.; Dekker: J. P. *Proc. Natl. Acad. Sci. U.S.A.* **1995**, *92*, 4798−4802.

(42) Löwdin, P.-O. *J. Chem. Phys.* **1951**, *19*, 1396−1401.

(43) Löwdin, P.-O. *J. Mol. Spectrosc.* **1963**, *10*, 12.

(44) Fidder, H.; Knoester, J.; Wiersma, D. A. *J. Chem. Phys.* **1991**, *95*, 7880−7890.

(45) Marguet, S.; Markovitsi, D.; Millie, P.; Sigal, H.; Kumar, S. *J. Phys. Chem. B* **1998**, *102*, 4697−4710.

(46) Dow, J. D. *Phys. Rev.* **1968**, *174*, 962.

(47) Hsu, C.-P.; Fleming, G. R.; Head-Gordon, M.; Head-Gordon, T. *J. Chem. Phys.* in press.

(48) Kühn, O.; Sundström, V. *J. Chem. Phys.* **1997**, *107*, 4154−4164.

(49) Chernyak, V.; Zhang, W. M.; Mukamel, S. *J. Chem. Phys.* **1998**, *109*, 9587−9601.

(50) Kimura, A.; Kakitani, T.; Tamato, T. *J. Phys. Chem. B* **2000**, *104*, 9276−9287.

(51) McConnell, H. *J. Chem. Phys.* **1961**, *35*, 508.

(52) Agagekyan, A. S. *Opt. Spectrosc.* **1970**, *29*, 37−40.

(53) Agebekyan, A. S. *Opt. Spectrosc.* **1971**, *30*, 247−250.

(54) Bodunov, E. N.; Malyshev, V. A. *Opt. Spectrosc.* **1979**, *46*, 271−275.

(55) Pullerits, T.; Freiberg, A. *Chem. Phys.* **1991**, *149*, 409−418.

(56) Beauregard, M.; Martin, I.; Holzwarth, A. R. *Biochim. Biophys. Acta* **1991**, *1060*, 271−283.

(57) McDermott, G.; Prince, S. M.; Freer, A. A.; Hawthorne-Lawless, A. M.; Papiz, M. Z.; Cogdell, R. J.; Isaacs, N. W. *Nature* **1995**, *374*, 517−521.

(58) Walla, P. J.; Linden, P. A.; Hsu, C.-P.; Scholes, G. D.; Fleming, G. R. *Proc. Natl. Acad. Sci. U.S.A.* **2000**, *97*, 10808−10813.